Multi-channel Spiral Twist Extrusion (MCSTE): A Novel Severe Plastic Deformation Technique for Grain Refinement

W.H. EL-GARAIHY, D.M. FOUAD, and H.G. SALEM

Multi-channel Spiral Twist Extrusion (MCSTE) is introduced as a novel severe plastic deformation (SPD) technique for producing superior mechanical properties associated with ultrafine grained structure in bulk metals and alloys. The MCSTE design is based on inserting a uniform square cross-sectioned billet within stacked disks that guarantee shear strain accumulation. In an attempt to validate the technique and evaluate its plastic deformation characteristics, a series of experiments were conducted. The influence of the number of MCSTE passes on the mechanical properties and microstructural evolution of AA1100 alloy were investigated. Four passes of MCSTE, at a relatively low twisting angle of 30 deg, resulted in increasing the strength and hardness coupled with retention of ductility. Metallographic observations indicated a significant grain size reduction of 72 pct after 4 passes of MCSTE compared with the as-received (AR) condition. Moreover, the structural uniformity increased with the number of passes, which was reflected in the hardness distribution from the peripheries to the center of the extrudates. The current study showed that the MCSTE technique could be an effective, adaptable SPD die design with a promising potential for industrial applications compared to its counterparts.

https://doi.org/10.1007/s11661-018-4621-4

I. INTRODUCTION

THE grain size of crystalline metals is regarded as a major microstructural aspect affecting both the mechanical and physical properties of a component. Inherently, controlling the grain size produces products with the desired properties. Accordingly, to cope with the never-ending race of tailoring materials with enhanced properties in service conditions, several attempts for the development of feasible grain-refinement techniques have been made and are still in progress.[1] Among these different approaches, the most successful has been the Severe Plastic Deformation (SPD), which has emerged as an effective technique for exposing materials to intensive plastic straining to achieve an ultra-fine-grained (UFG) structure.[2,3]

Currently, researchers are focusing on improving SPD methods tailored for the fabrication of various UFG materials, which exhibit superior properties that are valuable for different industrial applications.[4,5] SPD techniques, unlike conventional methods such as rolling, extrusion, forging, and drawing, refine grain size to the submicron scale and hence strengthen the material and enhance its mechanical properties without the need for introducing modification in the processed billet's dimensions.[1,2,6–8] The modification in the microstructure when adopting SPD techniques leads to a significant enhancement in functional, physical, chemical, and mechanical properties.[9] Consequently, the interest in SPD stems from the superior properties exhibited by the resultant UFG material.[10]

Currently, several alternatives of SPD techniques, which implicitly apply high hydrostatic pressure, are set for fabricating a wide range of materials. Among the most established renowned techniques are Equal Channel Angular Pressing (ECAP)[11–16] and High-Pressure Torsion (HPT),[17–21] which have proven to be very successful early implementations of the principles of SPD dating back to the early 1980s.[2] The ECAP works by pressing a metal rod through an angled channel, typically 90 deg. The process should be repeated several times to achieve optimal results, along with changing the orientation of the billet in each pass.[11] Therefore, the ECAP is considered as a discontinuous process, and for

W.H. El-GARAIHY is with the Mechanical Engineering Department, Unayzah College of Engineering, Qassim University, Qassim, 51911, Kingdom of Saudi Arabia and also with the Mechanical Engineering Department, Suez Canal University, Ismailia, 41522, Egypt. D.M. FOUAD and H.G. SALEM are with the Mechanical Engineering Department, The American University in Cairo, Cairo, 11835, Egypt. Contact e-mail: hgsalem@aucegypt.edu
Manuscript submitted October 5, 2017.
Article published online April 20, 2018

that reason, the HPT process was introduced. The latter process is conducted *via* applying severe compressive stresses on a disk to obtain a high frictional force, which results in shearing the disk by torsion all in a single operation.[2] Several researchers have regarded HPT as the most efficient grain-refinement method. However, it is limited to processing small coined samples ranging from 10 to 15 mm in diameter and 10 mm in thickness.[1] This drawback has hindered the applicability of such thoroughly researched technique outside the scope of laboratory experimentation.

The development of industrially compatible SPD techniques represents an appealing challenge for researchers in the field of structural material science. Consequently, various techniques were developed as an attempt to alleviate the previous limitations. Multiple Forging (MF),[22] Accumulative Roll Bonding (ARB),[23] and Twist Extrusion (TE) [24–29] are examples of the recently developed techniques. Among these methods, TE presents a rather promising SPD technique for commercial and industrial use.[5] The principle of TE processing is to extrude billets of any arbitrary cross section (except that of circular) with a profile consisting of two straight regions separated by a twist channel, with the main parameters defined as follows: twist slope angle (β) and rotation angle (α).[30] Thus, the specimen is twisted by a specific angle in one direction and then re-twisted to the same angle in the opposite direction while maintaining its original cross section. A comparison between TE and the two-aforementioned SPD techniques reveals that TE processing provides several advantageous features. Unlike ECAP, the presence of two shear planes in TE enables the attainment of higher strain values across the processed billet, which intensifies the overall deformation.[28] This advantage was validated in a study comparing the degrees of grain refinement achieved after processing pure copper *via* TE and ECAP. It was reported that finer grains were achieved as a result of TE processing, which subsequently led to better strength improvements.[31] Moreover, despite the capability of HPT to impose the highest strain, compared to other SPD techniques,[32] its application is limited to small sample sizes, which has hindered its uptake by industry. In contrast, TE has the capability of extruding relatively large billets.[32] Therefore, TE enjoys the benefits of both extrusion and torsion with large potential for industrial applications such as in the aerospace-engines industry.[5,33]

In the pursuit to integrate TE in industry, limiting issues such as tool cost prevail.[25,31] The fabrication of a customized die for each and every product dimension is economically unjustified. To that end, in order to alleviate the aforementioned limitations of the conventional SPD process and to capitalize on the many advantages of conventional TE, a novel design termed "Multi-channel Spiral Twist Extrusion (MCSTE)" is introduced in this study. Based on the principles of the TE technique, the new design provides a rather simple solution that saves cost and entices the uptake of such technology in the market.[34] The MCSTE die design provides several advantages such as (i) flexibility in scaling up the die for industrial scale production, (ii) ease of assembly, (iii) facilitation of multiple passes without removal of the billet from the disks, (iv) allowance of multiple passes without causing dimensional or shape changes, (v) use of stacked customized disks to allow for flexibility in varying both the height and cross section of the extrudates without changing the TE die, (vi) processing of billets *via* different twist slope angles (β) up to 40 deg, and (vii) ability to vary the applied backpressure during extrusion with variable magnitudes depending on the materials' properties.

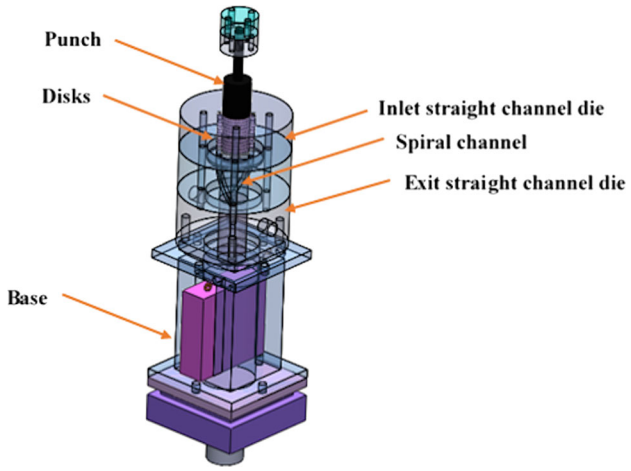

Fig. 1—Schematic illustration of MCSTE setup.

Accordingly, the current research work provides details on the novel MCSTE die design and demonstrates an assessment of the process. This is conducted through the characterization of the mechanical and microstructural behaviors of 1xxx series aluminum alloy billets processed up to 4 passes at a twist angle of 30 deg.

II. PRINCIPLES OF MCSTE

MCSTE is modified version based on the TE process. The die channel for MCSTE has three distinct channels: inlet, twist, and exit, as shown in Figure 1. In MCSTE, the inner geometry of the spiral die allows a square cross-sectioned billet within the stacked disks to twist about its longitudinal axis without undergoing dimensional or shape changes. Due to the specific design of the MCSTE die, the twisting direction of the billet within the inlet channel is 180 deg relative to the exiting channel. In other words, the billet twists about its longitudinal axis in a clockwise direction as it enters the die and in a counterclockwise direction as it exits. This feature allows the sample to be extruded repeatedly through the deformation and exit channels. Consequently, the imposed cumulative strain leads to the refinement of grains in the extrudate and hence influences its mechanical properties.

MCSTE can be used in processing ingot materials (IM), compact partially sintered powders, or canned green compact powders. For ingot materials, the billet is placed within a number of disks having a circular cross section with a diameter of 30 mm and thickness of

4 mm. The last disk is a solid to support the billet while passing through the three channels, as shown in Figure 2(a). A number of hollow disks, shown in Figure 2(b), having square cavities, are designed to host the billet to be processed. The shape and size of the hollow central section of the disk can be varied depending on the preselected dimensions of the billet. The disks are stacked above one another to cover the billet length. All disks have cylindrical addendums, with a diameter of 4 mm, to guide their motion along the different channels of the die, as demonstrated in Figures 2(a) and (b). The disks and billet are assembled in the first straight cylindrical channel with an internal diameter of 30 mm. Two opposite straight paths are present in the internal periphery of the straight channels to guide the disks' motion during processing.

In addition, the plunger used for IM (solid billets) has the same diameter as the disks. In the case of powder metallurgy (PM), the powder fills the internal cavity of the assembled disks, and the upper disk is closed using a stopper, which has the same geometry and dimensions as the internal cavity. After filling the disks' cavity with powder, the disks along with the powders are subjected to uniaxial hot compaction (hot pressing for simultaneous sintering) using a punch having the same geometrical shape as the disk cavity, as shown in Figure 2(c). Figure 2(d) shows a schematic drawing of the disks assembly and the used punch.

It is worth mentioning that the number of assembled disks governs the length of the processed billet. The manufactured setup of MCSTE can be used to process billets having lengths ranging from 1 to 80 mm, which is considered as a competitive feature of the MCSTE technique. Accordingly, varying the height of the MSCTE extrudates becomes effortlessly possible without the need for fabricating different die cavities with different dimensions. In addition, since the dimensions of the internal cavity of the disks control the dimensions of the processed billet, the MCSTE die has the ability of processing billets with different cross sections. This advantage helps in the investigation of the effect of the cross section of processed billets on the homogeneity of the produced mechanical properties and structure from the peripheries to the center.

For both IM and PM, the disk–billet assembly passes through the inlet channel through which the billet is subjected to compressive stresses (Figure 3(a)). The billet then undergoes excessive deformation passing through the twist channel. The disk–billet assembly is guided through the twist channel by the cylindrical addendum along two opposite spiral slots inclined with a twist slope of angle β with the vertical axis, as shown in Figure 3(b). Afterward, the assembly twists clockwise relative to the inlet channel and then undergoes a full counterclockwise rotation, through an angle (α) of 90 deg, as it passes through the exit channel of the die.

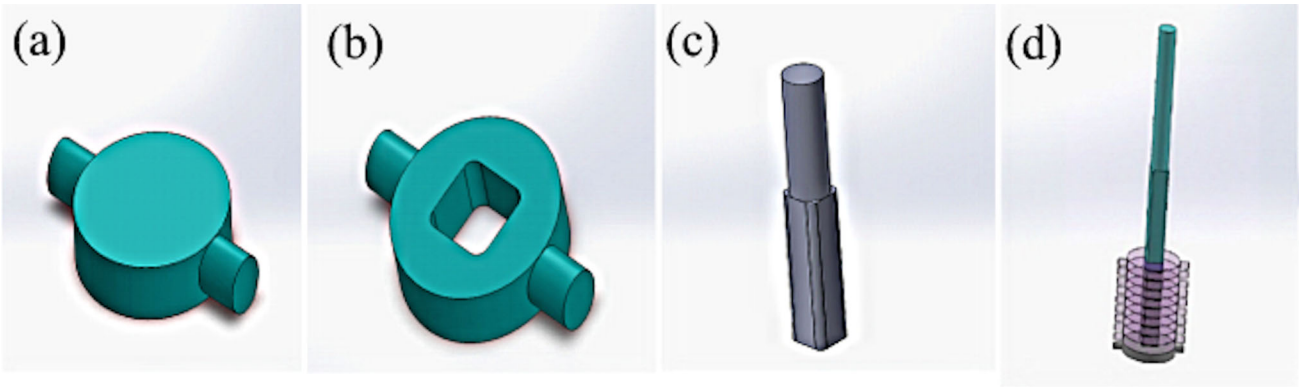

Fig. 2—Schematic illustrations of (*a*) solid disk with cylindrical addendums, (*b*) hollow disk, (*c*) punch, and (*d*) disks assembly.

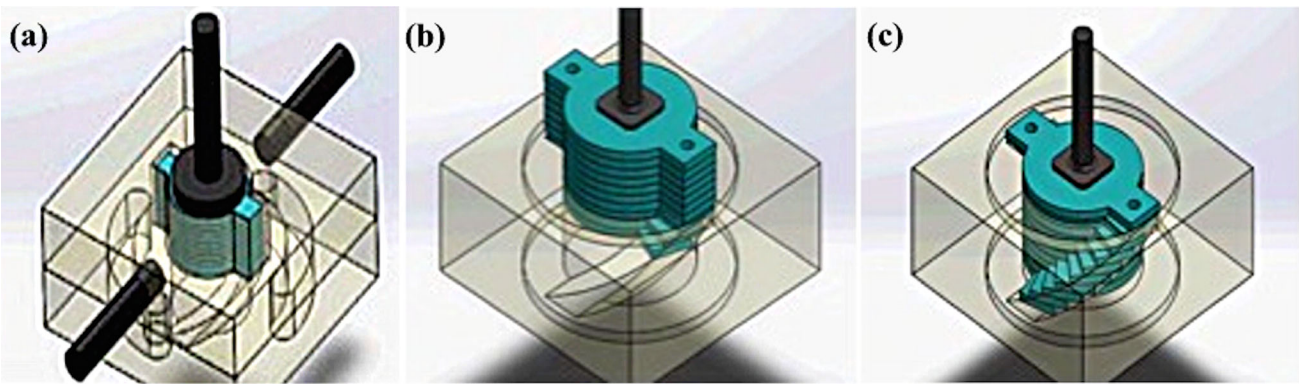

Fig. 3—Schematic drawing of MCSTE processing steps at (*a*) inlet channel, (*b*) twist channel, and (*c*) exit channel.

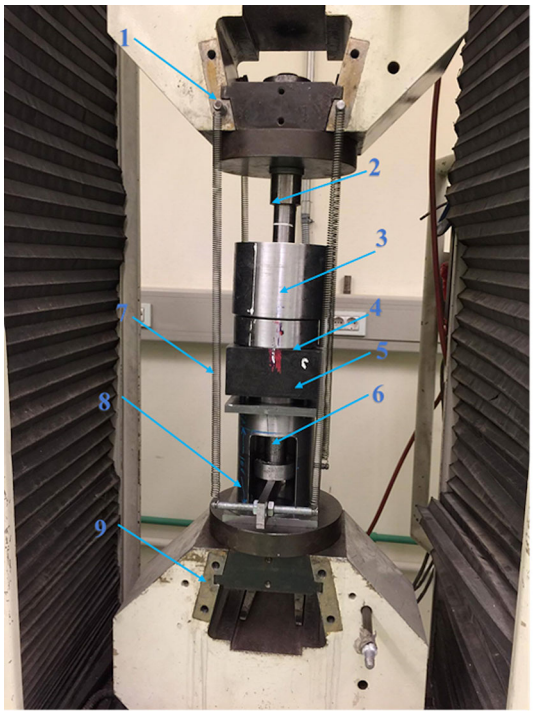

Fig. 4—MCSTE setup: (1) upper grip of testing machine, (2) pressing plunger, (3) inlet straight channel die, (4) twisted channel die, (5) exit straight channel die, (6) die base, (7) backpressure springs, (8) support plunger, and (9) lower grip of testing machine.

Accordingly, the billet is subjected to three stages of deformation: (i) compression at the inlet channel; (ii) clockwise shear deformation within the twist channel, in which the magnitude depends on the angle β within the twist channel; and (iii) counterclockwise shear deformation by twisting 90 deg within the exit channel.

In this study, the twist angle β was 30 deg. The three parts of the MCSTE die are assembled using four through-bolts to maintain the alignment between the die parts and to prevent any relative twisting between the MCSTE parts during processing. On the other hand, the three assembled parts of the die are fixed using four bolts to a hollow base, which is fixed to the universal testing machine. The die base, shown in Figure 4, contains a longitudinal cylindrical hole of 60 mm in diameter, in which a support plunger is housed. The function of the plunger is to support the assembled disks during the hot compaction process of the powder, which is carried out in the upper straight channel part of the die and prevents its motion during the compaction process. The support plunger is connected to the fixed part of the testing machine body using extension springs. Thus, the MCSTE disk–billet assembly is subjected to backpressure during processing. It is worth mentioning that another advantage of this technique is the possibility of changing the magnitude of the backpressure by increasing the number of used springs or replacing them with others having different stiffness values. After the completion of MCSTE processing, the connecting bolts are released to eject the processed billet using a plunger having the same geometry and dimension as the disk cavity.

Table I. Chemical Composition of AA1100 (Weight Percent)

Element	Fe	Cu	Mg	Mn	Al
Weight Percent	0.6	0.18	004	0.06	99

III. MATERIALS AND EXPERIMENTAL PROCEDURE

To validate the novel MCSTE die design as an SPD twist extrusion process, AA1100 billets 40 mm long with 10 × 10 mm square cross section were processed and characterized. The commercially pure AA1100 used in this work was received in the form of rectangular rods with the chemical composition as listed in Table I.

The experiments were performed at room temperature by means of 250 KN universal testing machine. The disk–billet assembly was pressed by means of a hardened steel plunger, subjected to a constant speed of 10 mm/min through the MCSTE die with a twist angle β (30 deg) which indicated a 90-deg rotation onto the cross section of the sample by the end of the 40-mm-long twist channel. Four MCSTE passes *via* route A were conducted, in which the billet was inserted into the entry channel without rotation between passes. The support plunger at the outlet of the exit channel, connected to extension springs, is used to create a minor backpressure (~ 5 MPa) against the disks motion during the extrusion process. Characterization of the billet was carried out for passes 1, 2, and 4, which were compared to the as-received (AR) plates (0-passes). Graphite-based lubricant was employed to reduce the friction between the disk–billet assembly and die inner walls (addendums and twist channel inclined slots) for each pass. Figure 5 demonstrates the billets before and after 1, 2, and 4-MCSTE passes.

To evaluate the influence of the MCSTE on the mechanical properties and microstructural evolution as a function of increasing the number of passes, the deformed billets were sectioned halfway along the billets' length to obtain a longitudinal cross section parallel to the extrusion direction. Vickers microhardness profiles were produced using a Mitutoyo HM112 testing machine with an applied load of 1 kg and dwell time of 15 seconds. Hv values were measured from the peripheries to the center on the billet sections cut parallel and perpendicular to the loading direction to evaluate the hardness variation across the billets' cross section. The displayed results are averaged over a minimum of five indentations per spot. Moreover, the hardness profiles and degree of homogeneity were depicted by color-coded contours developed to show the hardness distribution along the longitudinal and transverse directions of the MCSTE billet as a function of increasing number of passes. The tensile properties of the extruded billets as a function of increasing number of passes were characterized. Tensile specimens were

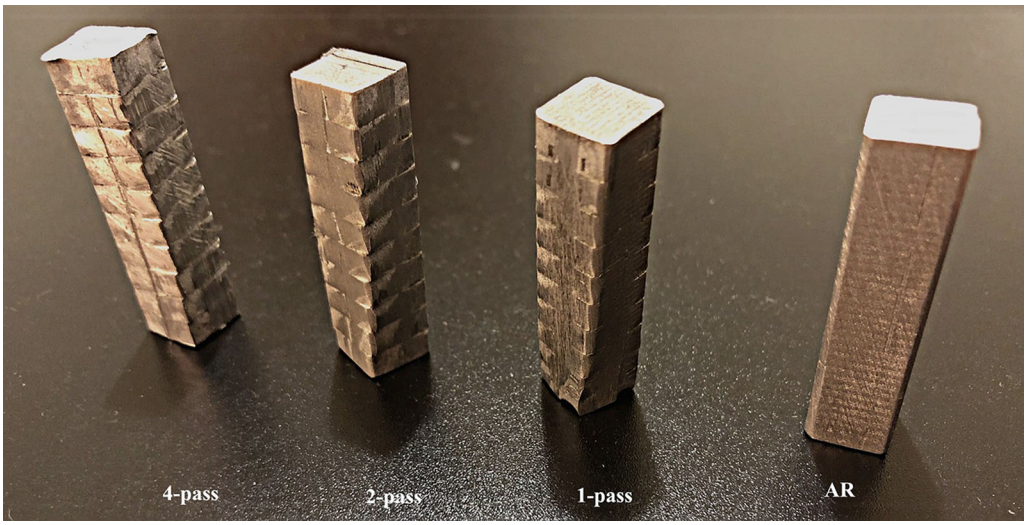

Fig. 5—Macrographs of MCSTE billets extruded with 0, 1, 2, and 4 passes *via* route A.

Table II. Mechanical Properties of the AA1100 Processed *via* MCSTE Compared to AR Plates

	Hv Values				
Processing Condition	Center	Periphery	Yield Strength (MPa)	Ultimate Tensile Strength (MPa)	Percent Elongation (Pct)
AR	30 ± 2	30 ± 2	55 ± 1	74 ± 1	24 ± 1
1-pass	43 ± 3.5	47 ± 1.75	60 ± 1	90 ± 2	23 ± 0.5
2-pass	47 ± 3	49 ± 3.5	80 ± 2	98 ± 3	23 ± 1
4-pass	50 ± 1	53 ± 1.5	98 ± 1	104 ± 1	22 ± 1

machined according to the American Society for Testing of Materials (ASTM) with a gage length of 24 mm and a diameter of 6 mm. A minimum of two tensile specimens were tested per condition using 100 kN Instron universal testing machine at a strain rate of 3 mm/min.

Optical microscopy (OM) (Leica DMIRM) was used to examine the microstructural evolution of the billets before and after 1, 2, and 4 MCSTE passes. The billets were prepared by sectioning using a high-precision IsoMet cutter. The sectioned billets were mechanically ground with silicon carbide papers up to 1200 grits, followed by polishing using alumina powder and etching using Flick's etchant. Finally, the average linear intercept method was employed to determine the average grain size as a function of increasing number of MCSTE passes.

IV. RESULTS AND DISCUSSION

A. *Microhardness*

Table II lists the average Vickers microhardness (Hv) measured at the peripheral and central regions of the AR plate and after MCSTE processing *via* 1, 2, and 4 passes. The hardness of the AR plate was uniformly distributed along the investigated cross section with an average value of approximately 30 Hv. As listed in Table II, hardness increased with the number of MCSTE passes, which could be attributed to the dominant effect of increasing dislocation density caused by strain hardening.[35] One-pass processing *via* MCSTE resulted in a 57 pct increase in the Hv values at the billet peripheral regions, while increasing the processing up to 4 passes resulted in a significant increase of 76.6 pct compared to the AR condition. The billets' central regions displayed 43.3 and 70 pct increases in the Hv value for the billets processed *via* 1 and 4 passes, respectively, compared to the AR condition. The reported higher Hv values at the peripheral regions compared to the central ones can be attributed to the induced high friction at the processing disk–billet interface, which increased the strain hardening effect at the peripheries compared to the center.[36] This can be clearly observed on the surfaces of the deformed billets as shown in Figure 5.

Figure 6 displays the hardness contours and Hv values recorded along the longitudinal cross section of the billets *vs* distance from each billet's central to peripheral regions. Similar plots are displayed for the transverse sections of the processed billet as shown in Figure 7.

From Figures 6(a) through (c), the hardness contours reveal increasing uniformity in properties with the increasing number of passes from 1 to 4, respectively. One MCSTE pass (Figure 6(a)) produced the lowest Hv values at the upper ends of the billet compared to the lower ends, which was consistent with the observations

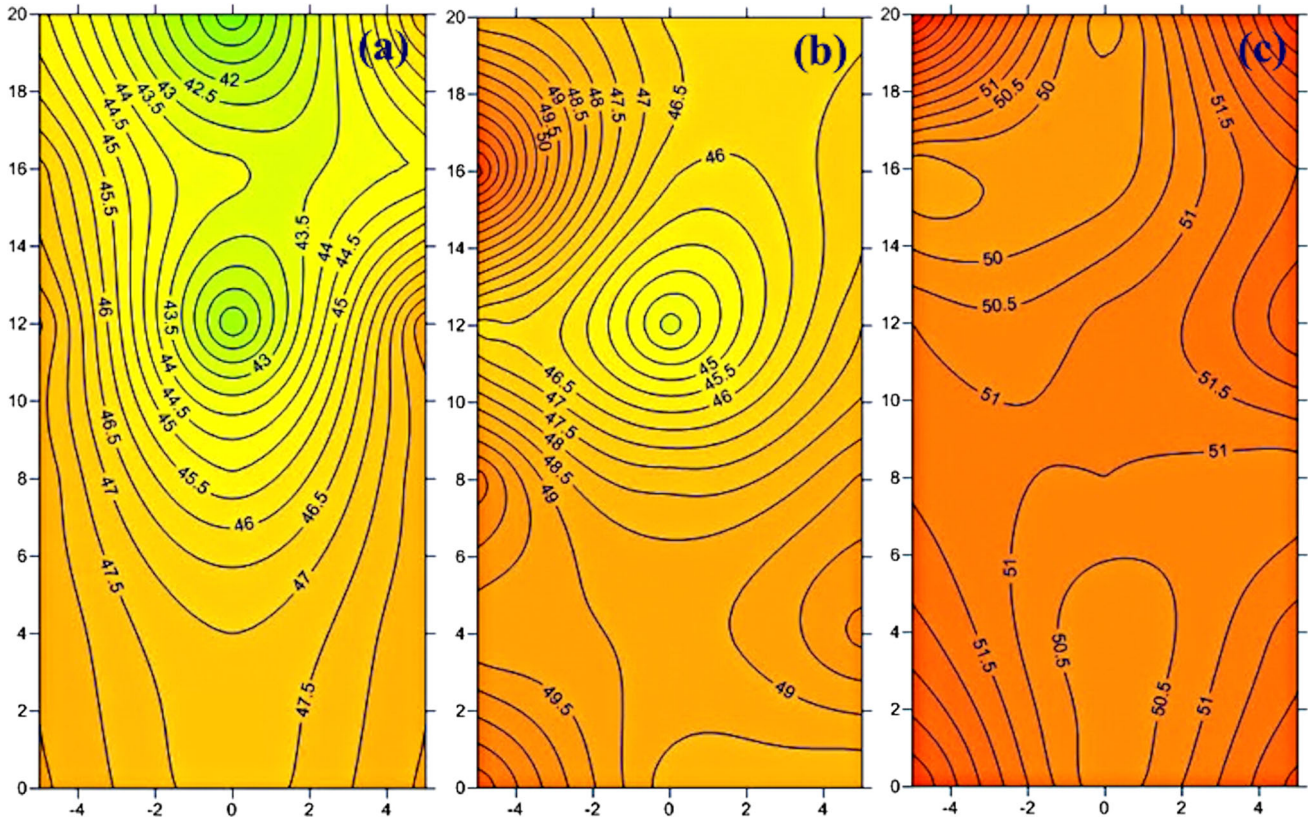

Fig. 6—Color-coded contour for the microhardness values recorded on the longitudinal planes of the billets processed *via* route A: (*a*) 1 pass, (*b*) 2 passes, and (*c*) 4 passes.

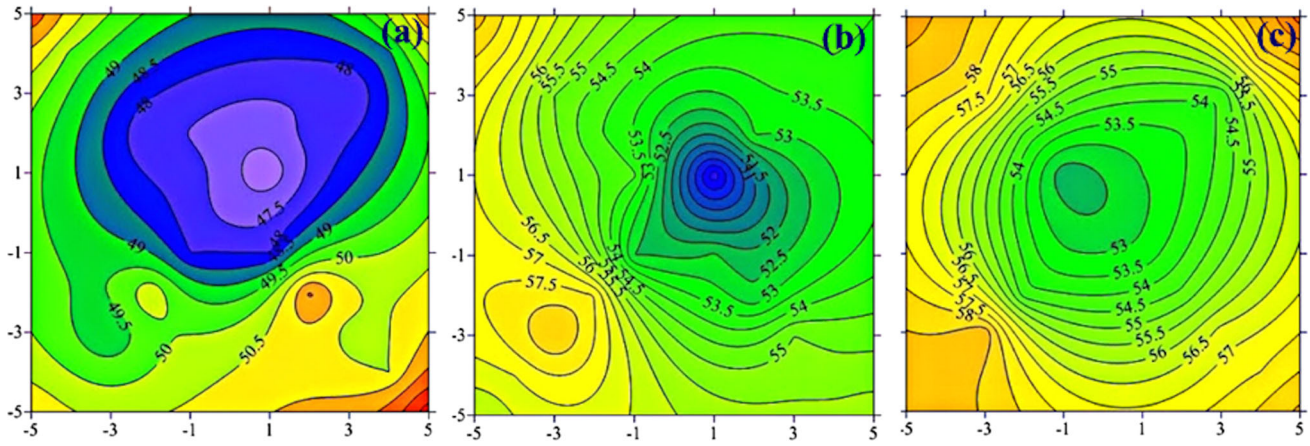

Fig. 7—Color-coded contour for the microhardness values recorded on the transverse cross sections of the billets processed *via* route A: (*a*) 1 pass, (*b*) 2 passes, and (*c*) 4 passes.

for the billets processed *via* 2 and 4 passes. This could be explained by the backpressure applied, which resulted in higher Hv values at the bottom section. It is possible that the billets were subjected to two types of resistance forces while passing through the MCSTE channels, the first generated at the transition from the inlet channel to the twisting channel, and the second could be generated by the backpressure springs. The former would be repeated as the bottom disk is forced to pass through the successive stages of the twisting channel until it passes through the exit channel. In this case, the billet would be subjected to an equivalent amount of strain throughout the twist channel. Meanwhile, the bottom part of the billet, *i.e.*, the lower disk, encounters a higher resistance to motion as a result of the backpressure springs. Thus, the lower disks would be forced to move forward to enter the exit channel while encountering the backpressure caused by the springs. Since the imposed

backpressure was relatively low, approximately 5 MPa, the induced strain hardening would have a short-range effect and only influence the lower part of the billet. Findings reported by Irania *et al.*[36] and Kim *et al.*[37] explained that the structural inhomogeneity of the TE billets increased when a backpressure over the range from 0 to 200 MPa was applied. Furthermore, higher Hv values were displayed at the peripheries of the billets' bottom surface, which decreased both toward the center and toward the top end. The Hv values ranged between 36 at the top central end and 48 at the bottom peripheral end. Two passes (Figure 6(b)) increased the relative uniformity of the hardness from the peripheries to the center of the billet along the longitudinal cross section compared to the first pass (Figure 6(a)), where the Hv values ranged between 45 at the center and 50 at the peripheries. On the other hand, billets processed up to 4 passes displayed Hv values ranging between 50 at the top central end and 53 at the bottom peripheral end (Figure 6(c)). This is indicative of increased uniformity of the deformation across the billets' cross section as the number of passes increases.

As shown in Figure 7, processing *via* 1 pass reveals 46.6 pct and 72.6 pct increases in the Hv values at the central and peripheral regions, respectively, compared to the AR conditions. This indicates a significant degree of inhomogeneity in the distribution of mechanical properties across the cross section of the billet, as shown in Figure 7(a). However, the hardness homogeneity across the billets' cross section increased with the increasing number of passes as shown in Figures 7(b) and (c), respectively. MCSTE 4-passes was associated with obvious increases in Hv values by 72 pct and 97.3 pct at the central and peripheral regions, respectively, compared to the AR conditions, which is consistent with the reported Hv results shown in Figure 6(c). The observed increase in hardness at the peripheries compared with the central regions is attributed to the nature of the torsional extrusion process. The higher strain imposed at the peripheral regions and the lower strain at the billet's central region depend on the billets' cross section; the larger the cross section, the higher the degree of strain inhomogeneity.[35] Based on the MCSTE die design (Figure 3), the billet is housed within a number of stacked disks; hence, the billet encountered variable strain distribution at the disk–billet interfaces (Figure 5). The maximum strain occurs at the disk–billet contact surfaces compared with the regions at the partition lines between the successively aligned disks. This phenomenon led to a relatively higher strain hardening at the periphery compared to that experienced at the central regions.[24,25] Zendehdel *et al.*[26] explained that the low Hv values at the central regions of billets processed at low strains are due to the insufficient amount of dislocations in these regions.

Moreover, despite the heterogeneous deformation across the billets' cross section, the intensity of the hardness variation tends to decrease with multiple MCSTE passes. As indicated in Table II and Figures 6(c) and 7(c), processing *via* 4 passes resulted in an enhancement of the deformation homogeneity both along the longitudinal (flow) and transverse cross sections. The isotropy in hardness distribution can attributed to the higher strains achieved by processing multiple passes, which led to the stabilization of the billet's internal structure. The shear stress associated with TE was transferred to the adjacent areas from the periphery to the center after the strain reached the saturation zone threshold.[27–29,38] The produced results for hardness were in good agreement with the findings of Bahadori *et al.*[28] and Orlov *et al.*[39] who reported similar increases in Hv values after 3 passes of TE of the same grade of aluminum alloy.

B. *Tensile Properties*

The engineering stress–strain (σ–ε) curves for the AR condition, as well as the processed specimens after 1, 2, and 4 passes *via* MCSTE, are shown in Figure 8. Table II lists the variations in yield, ultimate tensile strength, and elongation pct as a function of increase in the number of passes compared to the AR condition. The σ–ε curves revealed that imposing intense SPD, *via* the novel MCSTE process, resulted in a work-hardened material with enhanced yield and ultimate tensile strengths. This could be attributed to the multiplication of dislocations as a result of cold working and their interaction together. As illustrated, an increasing trend in the tensile properties was achieved with the increasing number of passes. From Table II, it is clear that an increase ranging from 9 and 22 pct was achieved in the yield strength (YS) and ultimate tensile stress (UTS), respectively, after 1 pass, and increasing the number of passes up to 4 passes was ensued by a significant increase of 78 and 41 pct in YS and UTS, respectively, compared to the AR condition.

On the other hand, a gradual decrease in the incremental rate of strengthening occurred as a function of increasing number of passes, where the increase in the UTS after 4 passes relative to that after 1 and 2 passes was 15 and 6 pct, respectively. Such behavior could be attributed to strain saturation, which is common for the 1xxx series aluminum alloys. After reaching a certain limit, minor effects on tensile properties could be achieved.[7,35] Similar findings were reported in.[40] The observed increase in UTS coupled with increasing the

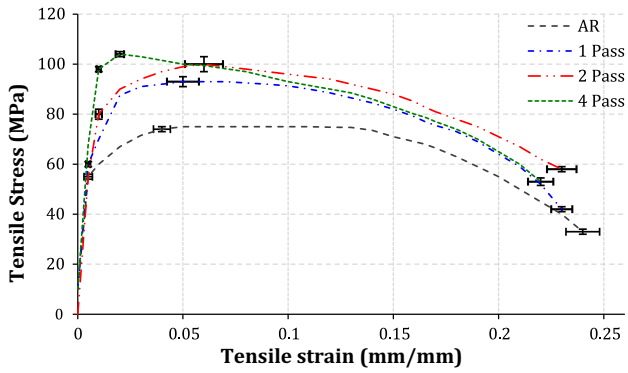

Fig. 8—Engineering σ-ε diagram for AA1100 billets processed by 1, 2, and 4 passes of MCSTE compared to the AR plates.

number of passes influenced the uniform and nonuniform strain compared to the AR condition. This could be attributed to the accumulation of strain after each pass, which resulted in increasing YS and UTS by strain hardening. In addition, the increased strength with increasing number of MCSTE passes was associated with an obvious retention of ductility, as depicted in Figure 8. One MCSTE pass had an insignificant influence on the uniform and nonuniform strain compared to the AR. However, increasing the number of passes to 4 resulted in decreasing the uniform strain region while retaining the nonuniform elongation percent (strain). This agrees with the Hv values measured both on the longitudinal (Figure 6) and transverse cross sections (Figure 7). This phenomenon could be related to the dynamic recovery in pure aluminum, which results in dislocation annihilation and absorption at the boundaries of the ultrafine grains.[35,41,42] This led to an increase in the ability of the material to accommodate additional deformation without a significant reduction in ductility.[35] Nonetheless, TEM analysis is necessary for further investigation of the influence of MCSTE passes on the internal structural evolution.

The enhancement in the mechanical properties achieved post MCSTE processing is higher than that achieved for AA1100 processed by other SPD techniques. A study by B. Leszcztnska-Madej *et al*. supports this claim, where an 80 pct increase in hardness was reported for pure aluminum after 16 ECAP passes compared to the 70 pct increase achieved after only 4 passes of MCSTE processing.[13,43] Furthermore, Horita et. al. reported a 40 pct increase in YS of AA1100 processed with 8 passes of ECAP at room temperature, which was accompanied by a 62 pct reduction in ductility.[44] Conversely, processing 4 passes *via* MCSTE increased YS by 78 pct and decreased ductility only by 2 pct. Accordingly, the displayed results are indicative of the ability of the MCSTE process as an SPD technique that could effectively produce strong/tough metals and alloys.

C. *Microstructural Evolution*

To investigate the validity of the MCSTE process, a comprehensive study was conducted to investigate the influence of multiple passes on the microstructural evolution and homogeneity of the processed alloy. From the displayed hardness contours (Figures 6 and 7), the intensity of deformation is higher at the disk–billet interfaces (peripheral regions) compared to the central regions. The AR, 1-pass, and 4-pass billet microstructures were assessed using OM. Figures 9 and 10 demonstrate the microstructures at the central and peripheral regions for the MCSTE billets processed with 1 and 4 passes compared to the AR plate, respectively. The AR plates' microstructure revealed relatively uniform coarse grains with an average size of 111 μm both at the center (Figure 9(a)) and the peripheries (Figure 10(a)), which agrees with the measured low Hv values and tensile properties.

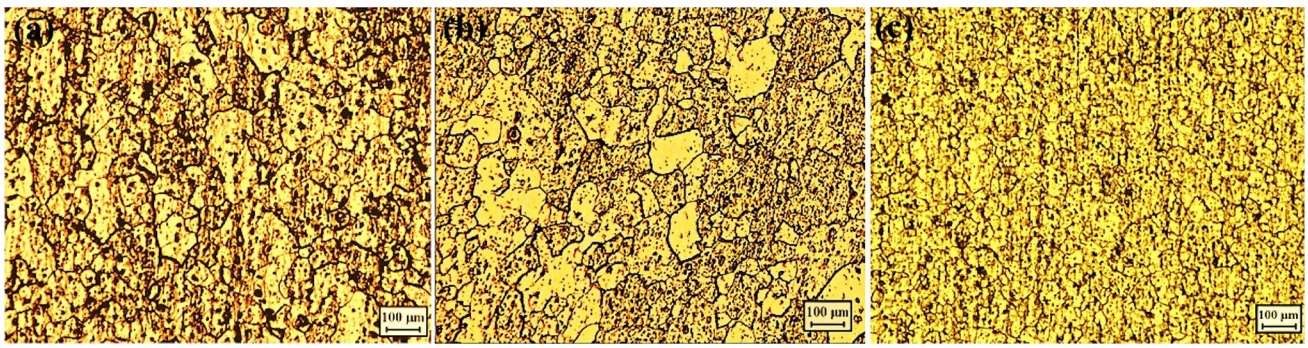

Fig. 9—OM micrographs of AA1100 central regions for (*a*) AR, (*b*) 1-pass and (*c*) 4-pass samples.

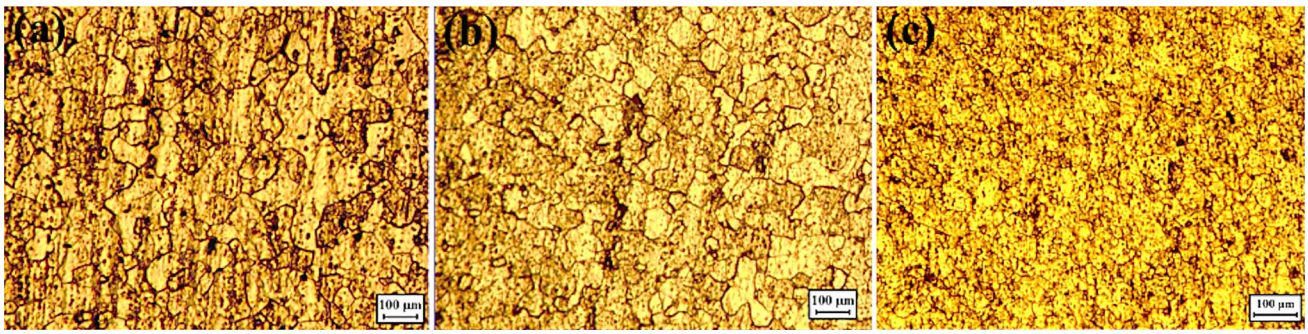

Fig. 10—OM micrographs of AA1100 at peripheral regions for (*a*) AR, (*b*) 1-pass and (*c*) 4-pass samples.

Table III lists the grain size variations in the samples after 1, 2, and 4 passes, measured both at the center and peripheries of the MCSTE billets. Increasing the number of MCSTE passes resulted in insignificant grain refinement at the center (Figures 9(b) and (c)) and peripheries (Figures 10(b) and (c)) for the billets processed with 1 and 4 passes, respectively. From the displayed results, the grain sizes of the AA1100 AR plates at the central regions were refined by 21, 29, and 68 pct after 1, 2, and 4 passes, respectively. Moreover, significant grain refinement was clearly manifested at the peripheries compared to the center of the MCSTE billets, as revealed in Figures 9 and 10. The average grain size at the center of the billet tends to be coarser compared to that at the peripheries, which agrees with the displayed hardness contours (Figures 6 and 7). The grain sizes at the peripheries of the billets were refined by 36, 38.7, and 72 pct, for the billets processed with 1, 2, and 4 passes, respectively.

After 1 pass of MCSTE, the microstructure was considerably refined but with a high degree of inhomogeneity due to the strain gradient imposed by the MCSTE. This is also revealed by the measured Hv values in Table II. The average grain size was reduced by 36 pct after the first pass reaching 70 μm in the peripheral region, while 21 pct refinement was measured at the center reaching 88 μm, as listed in Table III. The grain refinement at the peripheries (Figure 10(b)), compared to the central regions (Figure 9(b)) after 1 pass, could be attributed to the imposed high frictional forces induced at the disk–billet interface, which imposed higher shear stresses on the surface of the extrudates. The shear strain within the twist channel decreased from the peripheries to the center,[31,35] leading to a gradual decrease in grain refinement across the billet's cross section. Augmenting the intensity of plastic straining through MCSTE up to 4 passes led to significant grain refinements of 68 and 72 pct at the center compared to the peripheries, respectively. Consequently, increasing the number of passes resulted in enhancing the structural uniformity across the billets' cross section, as shown in Figures 8(c) and 9(c) and Table III.

In torsional strain, plastic shear gradients could result from the geometry of torsional deformation as radial augmentation of strain from the center to the periphery across the samples' cross section occurs.[24,25,45,46] In addition, the enhanced structural uniformity resulted in the corresponding uniformity in hardness distribution after 4 passes of MCSTE. Horita *et al.* proposed that the dislocation density proliferates as a function of severe deformation, forming subboundaries that hinder the dislocations movement at early stages of straining.[44] Multiple-pass processing gradually accumulates strain, resulting in an increase in grain misorientation and dynamic recrystallization that leads to finer grains of equiaxed microstructure.[27] As verified from the OM micrographs, the deformation occurs heterogeneously at the initial stages of the MCSTE processing. The inhomogeneity in strain distribution led to a nonuniform microstructure and grain refinement after the first 2 passes

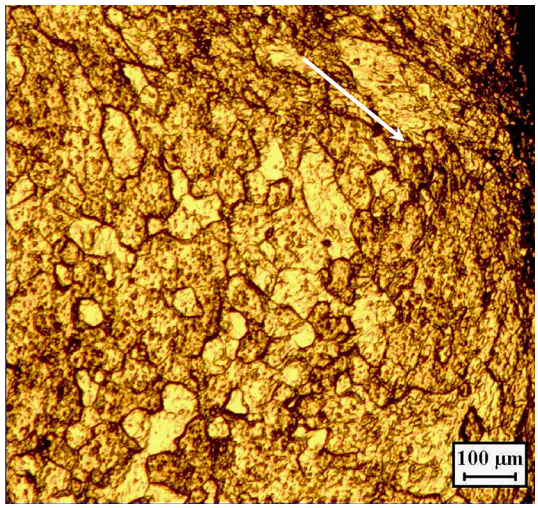

Fig. 11—OM micrograph of AA1100 after 1 pass at the peripheries (arrow represents the shear flow pattern).

of MCSTE processing (Figures 8(b), 9(b)). The decrease in heterogeneity of property distribution with the successive passes is attributed to the high intensity of stresses in the peripheral regions that oppose the new external stresses produced during TE processing. As a result, the stresses in these regions decreased. Conversely, in the central regions, the opposite is true, where the internal stress remaining from the first TE pass is lower than those at the corners, causing less decrease in the new external stresses during the successive TE passes.[47,48] Consequently, a homogenous distribution of strain across the microstructure prevails as depicted in Figures 9(c) and 10(c).

Notably, the grains at the peripheries of the processed billets *via* 1 and 4 passes, compared to the AR plates, were elongated in the direction of shear. The material flow pattern at the peripheries of the 1-pass sample along the longitudinal direction (flow direction) is shown in Figure 11, where the shear flow is indicated by the arrow. Moreover, evidence of the formation of internal structures was revealed by OM, where further investigation of the formed substructure using TEM analysis is required. However, it is suggested that the intense plastic deformation induced within the twist and the exit channels could be responsible for the formation of dislocation cells/subgrains near the peripheries of the extruded billets.[26,48]

Correspondingly, the evident enhancement in strength and hardness of the MCSTE processed billets could be attributed to the development of the homogeneous refined structure. According to the Hall–Petch law, the substantial grain refinement associated with SPD explains the increase in the hardness and strength of AA1100 billets, as shown in Table II.[49] The finer the grain size is, the higher the surface area of boundaries necessary for impeding the motion of dislocations.[8] It follows that the ultrafine substructure might have developed within the AR-sheared grains, which could be in the form of dislocation cells or subgrains depending on the misorientation angles.[8,49] Further

Table III. Average Grain Size Variation at the Central and Peripheral Regions of AA1100 MCSTE Billets Compared to the AR Plates

	Mean Grain Size (μm)			
Location	AR	1-Pass	2-Pass	4-Pass
Center	111	88 ± 3.5	84 ± 2.5	35 ± 1.5
Peripheries	111	70 ± 2	68 ± 3.5	31 ± 1

investigation is required using TEM to provide a comprehensive study of the structural evolution as a function of MCSTE passes and the influence of dynamic recovery associated with the intense plastic deformation.

V. CONCLUSIONS

A novel SPD process of MCSTE was designed, investigated, and validated. Based on the hardness contours, tensile behavior, and microstructural evolution, it could be concluded that the novel MCSTE design is a promising SPD technique suitable for processing ingot materials with superior mechanical properties. The results reported in this study, compared with those achievable *via* conventional SPD processes, showed that the MCSTE technique offers an effective, adaptable SPD technique with a promising potential for industrial applications.

1. The MCSTE processing at a relatively low twist angle (β) of 30 deg resulted in obvious increases in the hardness and tensile properties with the increasing number of passes which validates the ability of the process for imposing severe plastic deformation compared to its counterparts.
2. Deformation homogeneity increases with the increasing number of passes both on the longitudinal and transverse cross sections, yet the induced low backpressure could have prompted the increased hardness at the lower end of the billet.
3. Further studies are needed to produce a comprehensive structural analysis using TEM to further understand the influence of the MCSTE process on the structural evolution. In addition, studies are currently under way to investigate the influences of the increasing the number of passes beyond 4 passes and various β twist angles, routes, and strain hardenable alloys, as well as the billets' cross-sectional shapes and sizes.

ACKNOWLEDGMENTS

The authors would like to acknowledge the support extended by the Material Testing Laboratories in the Mechanical Engineering department, AUC by way of facilitating the use of the processing and testing equipment. Gratitude is also expressed to the Fresh Factory for Tools and Dies for their appreciable effort in manufacturing the MCSTE die.

REFERENCES

1. Y. Estrin and A. Vinogrado: *Acta Mater.*, 2013, vol. 61, pp. 782–817.
2. T.C. Lowe and R.V. Valiev: *JOM*, 2004, vol. 56, pp. 64–68.
3. H.J. Hu, Y.L. Ying, Z.W. Ou, and X.Q. Wang: *Mater. Sci. Eng. A*, 2017, vol. 695, pp. 360–66.
4. A. Fadaei, F. Farahafshan, and S. Sepahi-Boroujeni: *Mater. Des.*, 2017, vol. 113, pp. 361–68.
5. U.M. Iqbal, V.S. Senthil Kumar, and S. Gopalakannan: *Measurement*, 2016, vol. 94, pp. 126–38.
6. A. Farhoumand, P.D. Hodgson, and S. Khoddam: *J. Mater. Sci.*, 2013, vol. 48, pp. 2454–61.
7. M. Ebrahimi, H. Gholipour, and F. Djavanroodi: *Mater. Sci. Eng. A*, 2016, vol. 650, pp. 1–7.
8. M. Ensafi, G. Faraji, and H. Abdolvand: *Mater. Lett.*, 2017, vol. 197, pp. 12–16.
9. H. Sheikh, R. Ebrahimi, and E. Bagherpour: *Mater. Des.*, 2016, vol. 109, pp. 289–99.
10. M. Ebrahimi and M. Shamsborhan: *J. Alloys Compd.*, 2017, vol. 705, pp. 28–37.
11. Y. Duan, L. Tang, G. Xu, Y. Deng, and Z. Yin: *J. Alloys Compd.*, 2016, vol. 664, pp. 518–29.
12. Y.T. Zhu, T.G. Langdon, R.S. Mishra, S.L. Setniatin, M.J. Saran, and T.C. Lowe: *Ultrafine Grained Materials II*, Wiley, Hoboken, NJ, 2002, pp. 15–24.
13. B. Leszcztnska-Madej, M.W. Richert, and M. Perek-Nowa: *Arch. Metall. Mater.*, 2015, vol. 60, pp. 1437–40.
14. T. Hinklin and K. Lu: *Processing of Nanoparticle Structures and Composites*, Wiley, Hoboken, NJ, 2009, pp. 11–22.
15. K.I. Khodary, H.G. Salem, and M.A. Zikry: *Metall. Mater. Trans. A*, 2008, vol. 39A, pp. 2184–92.
16. A. Nassef, S. Samy, and W.H. ElGaraihy: *J. Mater. Metall. Eng.*, 2015, vol. 9, pp. 131–136.
17. H.G. Salem, W.H. El-Garaihy, and S. M. A. Rassoul: TMS 2012, Annu. Meet. Exhib., Suppl. Proc., 141st, Wiley, Hoboken, NJ, 2012, pp. 553–60.
18. W.H. El-Garaihy, S.M.A. Rassoul, and H.G. Salem: *Mater. Sci. Forum.*, 2014, vols. 783–786, pp. 2623–28.
19. A. Alhamidi, K. Edalati, and Z. Horita: *Mater. Res.*, 2013, vol. 16, pp. 672–78.
20. H.J. Lee, J.K. Han, S. Janakiraman, B. Ahn, M. Kawasaki, and T. Langdon: *J. Alloys Compd.*, 2016, vol. 686, pp. 998–1007.
21. M. Murashkin, I. Sabirov, D. Prosvirnin, and S. Dobatkin: *Metals*, 2015, vol. 5, pp. 578–90.
22. T.S. Naser and G. Krallics: *Acta. Polytech. Hungar.*, 2014, vol. 11, pp. 103–17.
23. S.O. Gashti, A. F-alhosseini, Y. Mazaheri, and M. Keshavarz: *J. Manuf. Proc.*, 2016, vol. 22, pp. 269–77.
24. M. Berta, D. Orlov, and P. Prangnell: *Int. J. Mater. Res.*, 2007, vol. 98, pp. 200–04.
25. D. Orlov, Y. Beygelzimer, S. Synkov, V. Varyukhin, N. Tsuji, and Z. Horita: *Mater. Trans.*, 2009, vol. 50, pp. 96–100.
26. H. Zendehdel and A. Hassani: *Mater. Des.*, 2012, vol. 37, pp. 13–18.
27. Y. Beygelzimer, A. Reshetov, S. Synkov, O. Prokofevea, and R. Kulagin: *J. Mater. Process. Technol.*, 2009, vol. 209, pp. 3650–56.
28. S.R. Bahadori, S.A. Mousavi, and A.R. Shahab: *Adv. Mater. Res.*, 2011, vols. 264–265, pp. 183–87.
29. D. Orlov, Y. Beygelzimer, S. Synkov, V. Varyukhin, N. Tsuji, and Z. Horita: *Mater. Sci. Eng. A*, 2008, vol. 519, pp. 105–11.
30. Sh.R. Bahadori, K. Dehghani, and S.A.A. Mousavi: *Mater. Lett.*, 2015, vol. 152, pp. 48–52.
31. S.V. Noor, A.R. Eivani, H.R. Jafarian, and M. Mirzaei: *Mater. Sci. Eng. A*, 2016, vol. 652, pp. 186–91.
32. Y. Beygelzimer, R. Kulagin, M. Latypov, and H. Kim: *Met. Mater. Int.*, 2015, vol. 21, pp. 734–40.

33. M.I. Latypov, E. Yoon, D. Lee, R. Kulagin, Y. Beygelzimer, M. Salehi, and H. Kim: *Metall. Mater. Trans. A*, 2014, vol. 45A, pp. 2232–41.
34. W.H. El-Garaihy, and H.G. Salem: Multi-Channel Spiral Twist Extrusion. Provisional Patent US 62/492,456.
35. F.J. Kalahroudi, A. Eivani, H. Jafarian, A. Amouri, and R. Gholizadeh: *Mater. Sci. Eng. A*, 2016, vol. 667, pp. 349–57.
36. M. Irania and M. Joun: *Russ. J. Non-Ferr. Met*., 2017, vol. 58 (6), pp. 632–38.
37. J. Gi Kim, M. Latypov, N. Pardis, Y.E. Beygelzimer, and H.S. Kim: *Mater. Des*., 2015, vol. 83, pp. 858–65.
38. A. Reshetov, A. Korshunov, A. Smolyakov, Y. Beygelzimer, V. Varyukhin, I. Kaganova, and A. Morozov: *Mater. Sci. Forum*, 2011, vols. 667–669, pp. 851–56.
39. D. Orlov, Y. Beygelzimer, S. Synkov, V. Varyukhin, N. Tsuji, and Z. Horita: *Mater. Sci. Eng. A*, 2009, vol. 519, pp. 105–11.
40. A. Eivani, M. Hosseini, H.R. Jafariah, and S.H. Mousavi: Anijdan, and N*Park*. *Mater. Charact*., 2017, vol. 130, pp. 204–2010.
41. D. Orlov, Y. Todaka, M. Umemoto, Y. Beygeelzimer, and N. Tsuji: *Mater. Trans*., 2012, vol. 53, pp. 17–25.
42. Y.T. Zhu and X. Liao: *Nat. Mater*., 2004, vol. 3, pp. 351–52.
43. Y.J. Li, W. Blum, and F. Breutinger: *Mater. Sci. Eng. A*, 2004, vols. 387–389, pp. 585–89.
44. Z. Horita, T. Fujinami, M. Nemoto, and T.G. Langdon: *Metall. Mater. Trans. A*, 2000, vol. 31A, pp. 691–701.
45. Q. Wei, S. Cheng, K.T. Ramesh, and E. Ma: *Sci. Eng. A*, 2004, vol. 387 ((1–2)), pp. 71–79.
46. Y.J. Li and W. Blum: *Phys. Stat. Solidi*, 2005, vol. 202, pp. R119–R121.
47. A. Molotnikov: *Mater. Sci. Forum*, 2008, vols. 584–586, pp. 1051–56.
48. S. Asghar, A. Mousavi, and S.R. Bahador: *JOM*, 2011, vol. 63, pp. 69–76.
49. A. Loucif, R.B. Figueiredo, T. Baudin, F. Brisset, R. Chemam, and T.G. Langdon: *Mater. Sci. Eng. A*, 2012, vol. 532, pp. 139–45.